



Effect of arrangement of carbon nanotube pillars on its gas ionization characteristics

Chia-Tsung Chang*, Chun-Yu Huang, Yu-Ren Li, Huang-Chung Cheng

Department of Electronics Engineering and Institute of Electronics, National Chiao Tung University, 1001 University Road, Hsinchu 300, Taiwan

ARTICLE INFO

Article history:

Received 26 December 2012
Received in revised form 24 February 2013
Accepted 25 February 2013
Available online 7 March 2013

Keywords:

Carbon nanotube (CNT) pillars
Gas ionization sensor (GIS)
Field enhancement factor
Breakdown voltage

ABSTRACT

The gas ionization sensors (GISs) using the carbon nanotube (CNT) pillars which has the pillar height (H) of 15 μm with interpillar spacing (R) of 30 μm as the cathode had been proposed for the first time to exhibit the 20 times higher field enhancement factor (β) and the lower breakdown voltage of 350 V with respect to the CNT film ones for nitrogen gas at the pressure of 0.035 Torr. As the H increased from 5 μm to 15 μm , the β increased with increasing the H since the electrical field could be enhanced via the aspect ratio increment. However, as the H increased from 15 μm to 60 μm , the β decreased with increasing the H owing to the increased field-screening effect. Such an optimum GIS with the CNT pillars also exhibited high sensitivity and selectivity for different kinds of gases detection as well as the good linearity for detecting the gas mixture.

© 2013 Elsevier B.V. All rights reserved.

1. Introduction

The sensing mechanism of the conventional semiconductor gas sensors based on the changes in the electrical properties of the semiconductor upon the exposure to gas. Since the same type gases exhibit the similar electrical properties, e.g. lower conductivities for all reducing gases and higher conductivities for all oxidizing gases, or vice versa. It caused that the gas sensors suffered from selectivity and reversibility issues [1]. Gas ionization sensors (GISs) had been introduced to overcome these problems because GISs could fingerprint the ionization characteristics of distinct gases. However, GISs were limited by the huge and bulky vacuum tube architecture, risky high-voltage operation, and high power consumption.

One-dimensional (1D) nanomaterials with high aspect ratio had attracted considerable attention in the fabrication of GIS because they could generate very high electric fields at relatively low voltages [2–7]. Among all 1D nanomaterials, carbon nanotubes (CNTs) were extensively owing to their relatively low work function, very sharp nanotips, and structural and chemical stability [4–7]. According to the previous research [4], the nanomaterial density effect on the field enhancement (FE) behavior played an important role to improve the gas ionization characteristics because the FE characteristics of CNTs might be influenced by the field-screening effect

from the proximity of neighboring CNTs. However, it was very difficult to exactly control the intertube distance for the CNT film. Therefore, it implied that the ratio of CNT height to intertube distance on the FE characteristics for the CNT films was very hard to be empirically realized. In recent years, the CNT pillars had been widely adopted for the field emission devices. The long and vertically aligned pillars with the exact control of the interpillar spacing (R) could be therefore practiced. However, the CNT pillars as the cathode were never demonstrated for the application in the GIS.

In this letter, the CNT pillars had been utilized for the first time to fabricate a GIS. As compared with the CNT film GIS, the CNT pillar ones exhibited the superior gas ionization characteristics, including sensitivity and selectivity for different kinds of gases detection as well as the linearity of the gas mixture. The pillar height effect of such CNT pillar GISs was also investigated.

2. Experiment

2.1. Fabrication of CNT pillar and film

At first, a 4 in. (100) p -type wafer was cleaned by the standard RCA cleaning process. Afterward, a photoresist was spin-coated on the Si substrate and the catalytic layer was defined by the mask which has the 50- μm -diameter circles with interspacing of 30 μm by photolithography. The 10-nm-thick aluminum, 1-nm-thick titanium, and 4-nm-thick co-deposition cobalt–titanium as the supporting, adhesion, and catalytic layers, respectively, were sequentially deposited on the photoresist-patterned Si substrate

* Corresponding author. Tel.: +886 35738343; fax: +886 35738343.
E-mail addresses: bgi815.ee96g@g2.nctu.edu.tw,
bgi815.ee96g@nctu.edu.tw (C.-T. Chang).

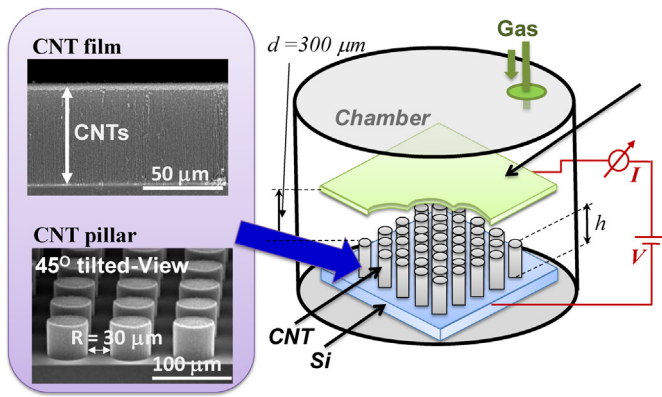


Fig. 1. Measurement setup of the gas ionization sensor. (Insets were FE-SEM images at the height of 60 μm: cross-sectional image of the CNT film and 45° tilted-view image of the CNT pillars.

through the magnetron sputtering system at room temperature. Then, the patterns were formed after removing the photoresist by lift-off method. Finally, the CNT pillars were grown on the patterned catalyst by the thermal CVD. The height of CNTs pillars were controlled to be 5, 10, 15, and 60 μm, accordingly, by tuning the synthesized time. Therefore, the diameter and the R of the CNT pillars were set as 50 μm and 30 μm, respectively. For comparison, the CNTs films with the same catalytic metal layers but unpatterned were also performed as the gas ionization sensor. The FE-SEM images exhibited the long vertically aligned CNTs for both the pillars and films, as shown in the inset of Fig. 1. Besides, the R of the CNT pillars could be precisely controlled.

2.2. The measuring system of gas ionization sensor

The gas ionization measurement setup was depicted in Fig. 1. An indium tin oxide was utilized as the anode and the CNT pillar or films acted as the cathodes. A distance d of 300 μm was kept between the anode and the tip of the CNTs for all measurements of various CNT structures. During the measurement, the sample was loaded into a vacuum chamber and the breakdown voltage (V_{br}) was measured in the target gas environment at different gas pressures. The anode voltage was applied with a source measurement unit (Keithley 237) while the cathode was biased at 0V (Keithley 238).

3. Results and discussion

3.1. Gas ionization characteristics

Fig. 2(a) shows the V_{br} as a function of the product of gas pressure, p , and distance between the anode and the tip of the CNTs, d , for the CNT films and pillars with different heights in nitrogen. The gas pressure was varied from 1.3×10^{-3} to 2.5×10^{-1} Torr. From Fig. 2(a), the CNT films exhibited only one curve since the d was fixed as 300 μm. It was observed that the similar trends of V_{br} curves were obtained for not only the CNT films but also the CNT pillars with different heights. From the Paschen's law, the relationship between the V_{br} curve and the $p \times d$ was dependent on the test gas. Since the testing gas was nitrogen, the trends of V_{br} curves should be similar for all CNT samples. But the CNT pillars with different heights exhibited different V_{br} 's for the same $p \times d$. As the pillar height (H) increased from 5 μm to 15 μm, the V_{br} curve decreased with increasing the H . However, as the H increased from 15 μm to

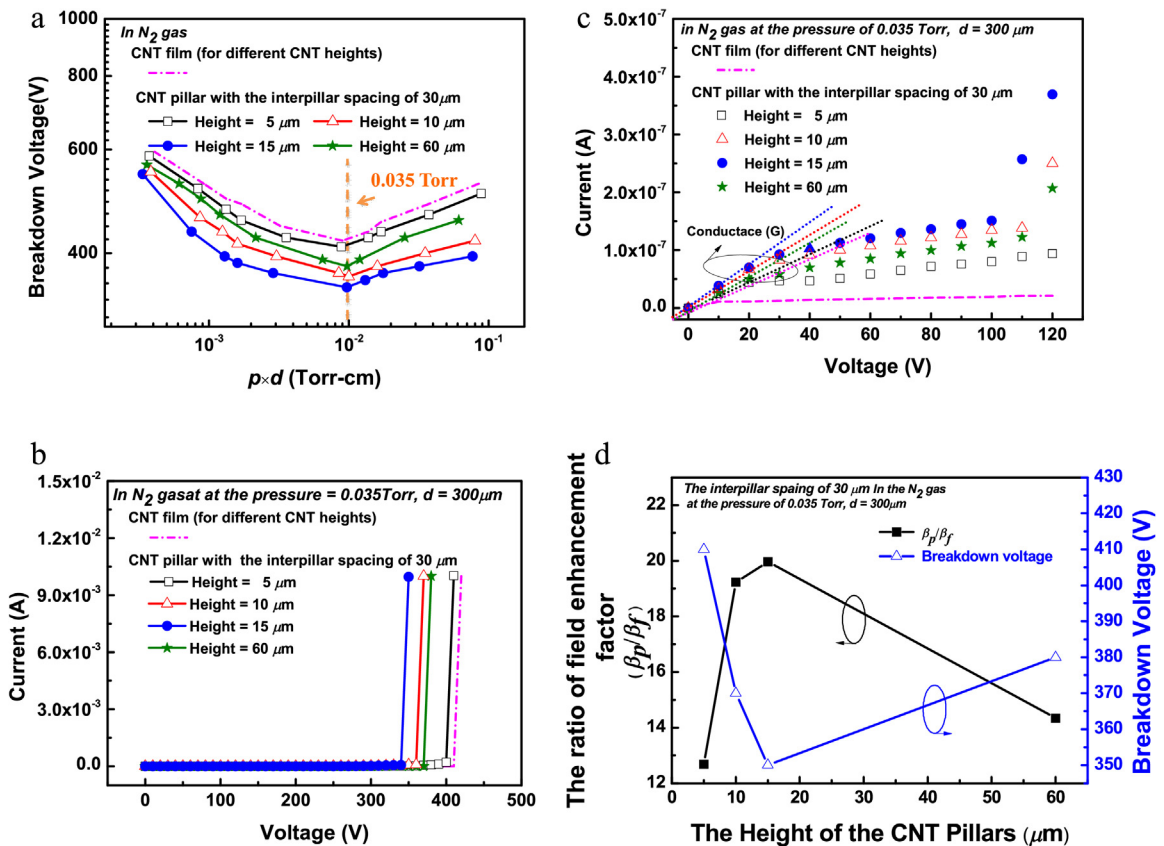


Fig. 2. Gas ionization characteristics at the pressure of 0.035 Torr in nitrogen: (a) V_{br} as a function of the $p \times d$ for the CNT film and different pillar heights. (b) Gas I - V characteristics for the CNT film and different pillar heights. (c) Pre-breakdown characteristic of the CNT film and pillars with different pillar heights. (d) β_p/β_r and V_{br} as a function of the height of the CNT pillars.

60 μm , the V_{br} curve increased with increasing the H . Moreover, the V_{br} 's had the minima as the $p \times d$ approached 10^{-2} Torr cm (i.e., the gas pressure was equal to 0.035 Torr at the fixed d of 300 μm).

To further realize the V_{br} variation with the different H , the gas pressure for the lowest breakdown voltage, namely 0.035 Torr, was therefore adopted. The current–voltage (I – V) characteristics for all the GISs in nitrogen gas at the gas pressure of 0.035 Torr were shown in Fig. 2(b). The V_{br} 's of the CNT pillar GISs were 410, 370, 350, and 380 V for the H of 5, 10, 15, and 60 μm , respectively. In contrast, the V_{br} of the CNT film ones was 420 V. Therefore, the proposed CNT pillar GISs exhibited the better characteristics than the CNT film ones. Furthermore, the structure of the CNT pillars with the H of 15 μm had the lowest V_{br} in all CNT pillars with different heights. It was conjectured the influence of the H on the FE characteristics of the CNT pillars GIS.

3.2. Field enhancement effect of the cathode CNT pillars and their aspect ratio

Consequently, the FE factors of all CNT GISs were further discussed. Fig. 2(c) shows the pre-breakdown characteristics of GISs for the CNT films and pillars with different heights. In addition, the effective conductance G of the devices could be determined by the slope of the ohmic region of the I – V characteristics, as the dash dot in Fig. 2(c). It was evident that all the effective conductance of the CNT pillar GISs, G_{p} , were higher than the CNT film ones, G_{f} . Moreover, the CNT pillar GIS with the H of 15 μm had a maxima effective conductance among all CNT pillar ones.

For the typical gas I – V characteristic, the current density was determined by the carriers travel speed as the electric field was very small and could be therefore expressed as [7]

$$J = \sigma_{\text{gas}} E_{\text{eff}} = \sigma_{\text{gas}} \beta E_{\text{app}} \quad (1)$$

where σ_{gas} was the gas conductivity, E_{eff} was the effective enhanced field at the tip vicinity, and E_{app} was the applied electric field between the electrodes. According to Eq. (1), the current densities in the CNT film and pillars could be obtained as

$$J_{\text{f}} = \sigma_{\text{gas}} \beta_{\text{f}} E_{\text{app}} \text{ and } J_{\text{p}} = \sigma_{\text{gas}} \beta_{\text{p}} E_{\text{app}}, \quad (2)$$

where J_{f} and J_{p} were the current density of the CNT film and pillars, as well as β_{f} and β_{p} were the FE factor of the CNT film and pillars. Since all of the devices were examined in the same chamber for the same test gas, so the σ_{gas} would be the same. Then, the ratio of the J_{p} and J_{f} could be written as

$$\frac{J_{\text{p}}}{J_{\text{f}}} = \frac{\beta_{\text{p}}}{\beta_{\text{f}}} \quad (3)$$

From the ratio of the G_{p} and G_{f} could be written as the

$$\frac{G_{\text{p}}}{G_{\text{f}}} = \frac{I_{\text{p}}/V_{\text{p}}}{I_{\text{f}}/V_{\text{f}}} = \frac{J_{\text{p}}A_{\text{p}}/E_{\text{app}}d}{J_{\text{f}}A_{\text{f}}/E_{\text{app}}d} = \frac{\beta_{\text{p}}}{\beta_{\text{f}}} \times \frac{A_{\text{p}}}{A_{\text{f}}}, \quad (4)$$

where A_{f} and A_{p} were the areas for the CNT film and CNT pillars, respectively. As a result, the $\beta_{\text{p}}/\beta_{\text{f}}$ were equal to the $G_{\text{p}}/G_{\text{f}}$ owing to the $A_{\text{f}} \approx A_{\text{p}}$. Fig. 2(d) shows the $\beta_{\text{p}}/\beta_{\text{f}}$ and the V_{br} as a function of the H at the pressure of 0.035 Torr in nitrogen. The $\beta_{\text{p}}/\beta_{\text{f}}$ of the CNT pillars were about 12.5, 19, 20, and 14.5 V with respect to the H of 5, 10, 15, and 60 μm . As the H increased from 5 μm to 15 μm , the β increased with increasing the H since the electrical field could be enhanced via the aspect ratio increment. However, as the H increased from 15 μm to 60 μm , the β decreased with increasing the pillar heights owing to the increased field screening effect. Therefore, the $\beta_{\text{p}}/\beta_{\text{f}}$ exhibited the maximum at the H of 15 μm . By the way, the V_{br} had thus a minimum at the H of 15 μm for the R of 30 μm .

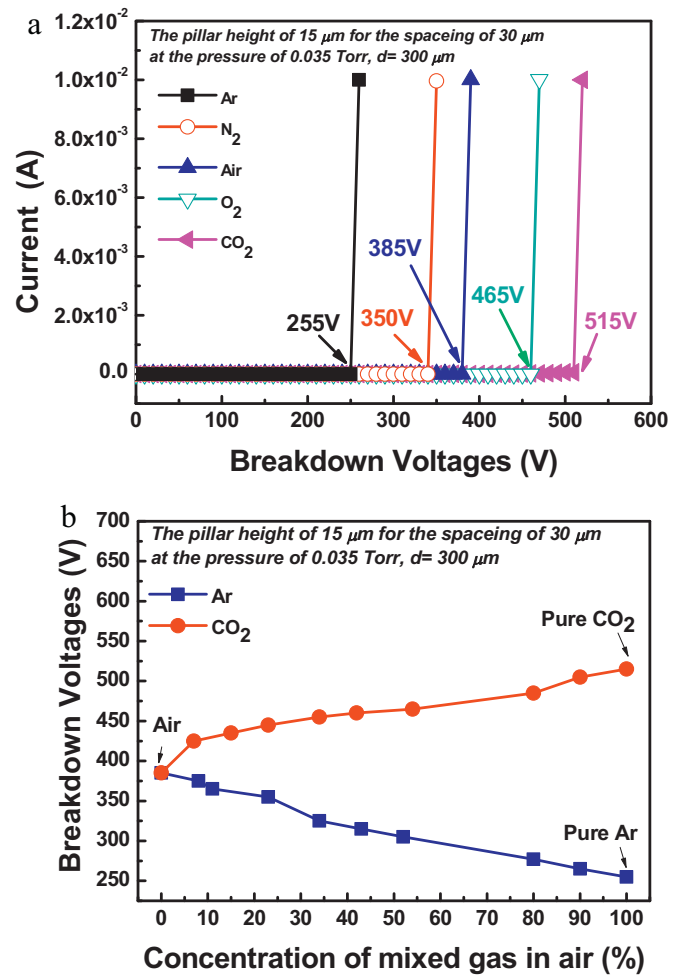


Fig. 3. (a) Gas I – V characteristics of the CNT pillars at the H of 15 μm for the five single gases as the pressure was 0.035 Torr. (b) V_{br} of Ar–air and CO₂–air gases in mixture as a function of gas concentration as the pressure was 0.035 Torr.

3.3. Single gas and gas mixture detection

Furthermore, the optimal CNT pillar GIS, which was at the H of 15 μm and the R of 30 μm , was used to distinct the different gases and detect the gas mixture at the pressure of 0.035 Torr. The I – V characteristics of the CNT pillar GIS for five single gases are shown in Fig. 3. From Fig. 3(a), the gas variety could be identified. Moreover, Argon (Ar) gas displayed the lowest V_{br} of 255 V and carbon dioxide (CO₂) gas showed the highest V_{br} of 515 V. Although the V_{br} depended mainly on the intensity of electric field and the bonding energy of the gas molecules [8], the numerical order of the V_{br} of the detected gases would be influenced by the selection of the $p \times d$ value. Therefore, it caused that the numerical order of the V_{br} were shown as Ar (225 V) < N₂ (350 V) < air (385 V) < O₂ (465 V) < CO₂ (515 V) in this manuscript. Fig. 3(b) shows the V_{br} of Ar–air and CO₂–air gases in mixture as a function of gas concentration. Obviously, the V_{br} increased with increasing CO₂ concentration. In contrast, the V_{br} decreased with increasing Ar concentration. This was because air had a higher V_{br} than Ar and lower V_{br} than CO₂, so the presence of air molecules tended to impede the breakdown of Ar and assist the breakdown of CO₂. Both two cases exhibited the good linearity to compare with previous researches [5,6]. The experimental results showed that the optimum arrangement CNT pillars were more effective for the application in GIS.

4. Conclusion

The superior ionization characteristics of the GIS had been proposed for the first time via the vertical-aligned CNT pillars as the cathode to exhibit the 20 times higher β and the lower V_{br} of 350 V for the H of 15 μm and the R of 30 μm with respect to the CNT film ones for the nitrogen gas at the pressure of 0.035 Torr. As the H increased from 5 μm to 15 μm , the β increased with increasing the H since the electrical field could be enhanced via the aspect ratio increment. However, as the H increased from 15 μm to 60 μm , the β decreased with increasing the pillar heights owing to the increased field screening effect. Such an optimum GIS with the CNT pillars also exhibited high sensitivity and selectivity for different kinds of gases detection as well as the good linearity for detecting the gas mixture.

Acknowledgments

This work was supported by the National Science Council of the Republic of China under the Grant Number NSC 101-2221-E-009-077-MY3, and in part by the Nano Facility Center of National Chiao Tung University, and National Nano Device Laboratories (NDL) for providing process equipment.

References

- [1] S.J. Gentry, T.A. Jones, The role of catalysis in solid-state gas sensors, *Sensors and Actuators* 10 (1986) 141–163.
- [2] Z. Fan, D. Wang, P. Chang, W. Tseng, J.G. Lua, ZnO nanowire field effect transistor and oxygen sensing property, *Applied Physics Letters* 85 (2004) 5923–5925.
- [3] Z. Liu, P.C. Searson, Single nanoporous gold nanowire sensors, *Journal of Physical Chemistry B* 110 (2006) 4318–4322.
- [4] S. Mahmood, Z.A. Burhanudin, N.H. Hamid, Effect of CNT density variation in field emission model of ionization gas sensor, in: *IEEE Regional Symposium Conf. on Micro and Nanoelectronics (RSM)*, 2011, pp. 266–269.
- [5] G. Hui1, L. Wu, Min Pan, Y. Chen, Li. Ting, X. Zhang, A novel gas-ionization sensor based on aligned multi-walled carbon nanotubes, *Measurement Science & Technology* 17 (2006) 2799–2805.
- [6] A. Modi, N. Koratkar, E. Lass, B. Wei, P.M. Ajayan, Miniaturized gas ionization sensors using carbon nanotubes, *Nature* 424 (2003) 171–174.
- [7] R.B. Sadeghian, M. Kahrizi, A novel miniature gas ionization sensor based on free-standing gold nanowires, *Sensors and Actuators A-Physical* 137 (2007) 248–255.
- [8] Y. Wang, J.T.W. Yeow, A review of carbon nanotubes-based gas sensors, *Journal of Sensors* 2009 (2009) 493904–493928.

Biographies

Chia-Tsung Chang was born in 1983. He received the BS degree in Electrical Engineering from Chinese Culture University in 2005 and MS degree in Electrical Engineering from National Central University in 2007. He is presently a PhD student at the Department of Electronics Engineering in National Chiao-Tung University. His research interests include fabrication and characterization of field emission device and gas ionization sensor.

Chun-Yu Huang was born in 1987. He received the BS and MS degrees in Electronics Engineering from National Chiao-Tsung University in 2009 and 2011. His research mainly focused on improvement the gas ionization sensor with carbon nanotubes.

Yu-Ren Li was born in 1987. She received the BS degree in physics from National Cheng-Kung University in 2009. She is direct admission from the MS degree into the doctoral programs in Electronics Engineering from National Chiao-Tsung University. Her research focused on nanomaterial, nanodevice and sensitive technology.

Huang-Chung Cheng is a professor of Department of Electronics Engineering in National Chiao-Tung University. He received the BS degree in physics from National Taiwan University in 1977, and the MS and PhD degrees from the Department of Materials Science and Engineering, National Tsing-Hua University, Hsinchu, Taiwan, in 1979 and 1985, respectively. He has published nearly 500 technical papers in international journals and conferences, and also held more than 50 patents. His current research interests are in the areas of high-performance TFTs, novel nanowire devices, non-volatile memories, three-dimensional integrations, novel field emission displays, biosensors, and photoelectronic device.